

Polymerization mechanism and conformation of poly(1-butene)

Tetsuo Asakura, Makoto Demura and Kaoru Yamamoto

*Department of Polymer Engineering, Tokyo University of Agriculture and Technology,
Nakamachi 2-chome, Koganei, Tokyo 184, Japan*

and Riichirō Chûjō

*Department of Polymer Chemistry, Tokyo Institute of Technology, 12-1 Ookayama,
Meguro-ku, Tokyo 152, Japan*

(Received 30 June 1986; revised 3 October 1986; accepted 13 October 1986)

Assignment of the ^{13}C nuclear magnetic resonance spectrum of poly(1-butene) to microtacticity was performed from previously calculated chemical shift data and confirmed from the excellent agreement of the relative intensities of each of four carbon peaks. The polymerization mechanism was successfully interpreted in terms of the bicatalytic sites model. The bond probabilities of the 6–11 bonds were calculated for 2,4,6,8,10,12,14,16,18-nonaethylnonadecane, a model compound of poly(1-butene), and compared with those of 2,4,6,8,10,12,14,16,18-nonamethylnonadecane, a model compound of polypropene.

(Keywords: poly(1-butene); ^{13}C nuclear magnetic resonance γ effect; rotational isomeric state model; tacticity; bicatalytic sites model)

INTRODUCTION

So far, n.m.r. chemical shift calculations concerning polymer microtacticity have been performed with the main object being to interpret the peaks, which have already been assigned to tacticity in connection with the time-averaged conformation, rather than to consider the method of assignment¹. However, agreement between calculated and observed ^{13}C n.m.r. peaks was very good, especially for olefin polymers using calculations based on the ^{13}C n.m.r. γ effect on the chemical shift and the application of the rotational isomeric state (r.i.s.) model to the polymer conformation^{2–5}. Such chemical shift calculations are, therefore, reliable for the assignment of the splitting of the peaks due to microtacticity. Based on the agreement between the calculated and observed chemical shifts, we can perform analyses with the time-averaged polymer conformation in solution along with the bond probabilities obtained from the r.i.s. model.

In this paper, the relative intensity of each ^{13}C n.m.r. peak will be determined for poly(1-butene) (PB). Simulation will be used under the assumption of a Lorentzian shape⁶. Peak assignment to microtacticity will be performed from previously calculated chemical shift data⁴ and confirmed from the excellent agreement of the relative intensities of each of four carbon peaks in PB. The polymerization mechanism will be examined based on the peak intensities at the pentad level. Moreover, the bond probabilities determined for PB will be summarized and compared with those determined for polypropylene (PP).

CALCULATION

The ^{13}C n.m.r. spectrum of predominantly isotactic PB reported previously⁷ was used for a comparison with the

calculated data. Details of the sample preparation and n.m.r. observation conditions are described elsewhere⁷.

Spectral simulation assuming a Lorentzian was done iteratively using peak positions, peak heights, widths at half-height, trough positions and trough heights⁶. In the examination of the bicatalytic sites model of Pino⁸ applied to the analysis of PP polymerization mechanism⁹, the pentad relative intensities of PB were calculated iteratively to the observed data until the mean-square deviations became a minimum with a simplex algorithm¹⁰. Methods for the calculation of the bond probabilities are described elsewhere⁴.

RESULTS AND DISCUSSION

Figure 1a shows the observed and simulated ^{13}C n.m.r. spectra of the methylene carbon in the backbone chain of PB, together with the decomposed spectra assuming a Lorentzian shape. The stick spectra calculated are also shown⁴. The fractions of meso and racemic dyads were determined from the relative intensities in the resonance region split into two peaks, although a slightly asymmetric racemic peak implies the appearance of tetrad splitting. The origin of such small splitting due to the dyad tacticity observed in the methylene backbone is compensation of the shielding effect between the backbone carbon and side-chain carbons⁴. This is in contrast to the ^{13}C n.m.r. spectrum of the methylene backbone carbon of PP, where the peak splitting due to hexad⁴ expanded over 2.5 ppm. The fraction of meso is 0.753, which leads to isotacticity of this PB sample.

The ^{13}C n.m.r. spectrum of the methylene carbon of the side chain makes it possible to evaluate the pentad tacticity of the PB chain as shown in Figure 1b. On the basis of the ^{13}C n.m.r. chemical shift calculation of PB

reported previously⁴, the pentad assignment was readily performed. The only overlapped pentad peak is rmmr + mmrr; however, the individual intensities can be evaluated with the aid of the following relations¹¹:

$$\text{mmmr} + 2\text{rmmr} = \text{mmrm} + \text{mmrr}$$

$$\text{mrrr} + 2\text{mrrm} = \text{rrmr} + \text{mmrr}$$

The individual pentad intensities are listed in Table 1 as well as the tacticities obtained from other carbon peaks.

The peaks of the methyl carbon of the side chain were also assigned to pentad on the basis of chemical shift calculation (Figure 2a). Although greater overlap of the pentad peaks was observed than for the methylene carbon of the side chain, the pentad intensities evaluated from the peak simulation are in excellent agreement with each

other, as summarized in Table 2. This fact indicates the validity of our peak assignment.

The methine carbon peaks were assigned to triad, partially pentad, as shown in Figure 2b. The relative intensities were determined and are listed in Table 1. The dyad, triad and pentad intensities were, therefore, evaluated from the methylene (main chain), methine (main chain) and methylene (side chain) carbon resonances, respectively. The tacticities of PB determined

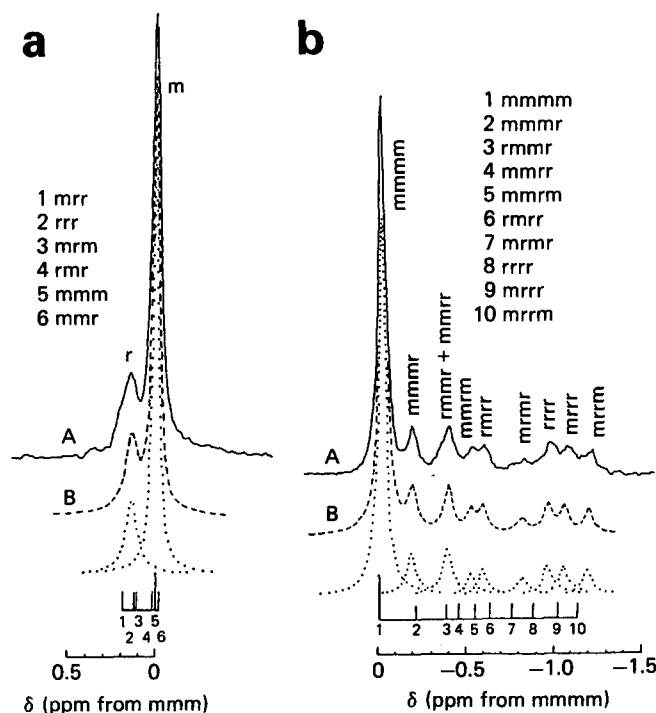


Figure 1 ¹³C n.m.r. spectra of methylene carbon of the backbone (a) and the side chain (b) of PB: A, observed spectrum; B, simulated spectra assuming Lorentzian. The stick spectrum calculated theoretically is also included⁴

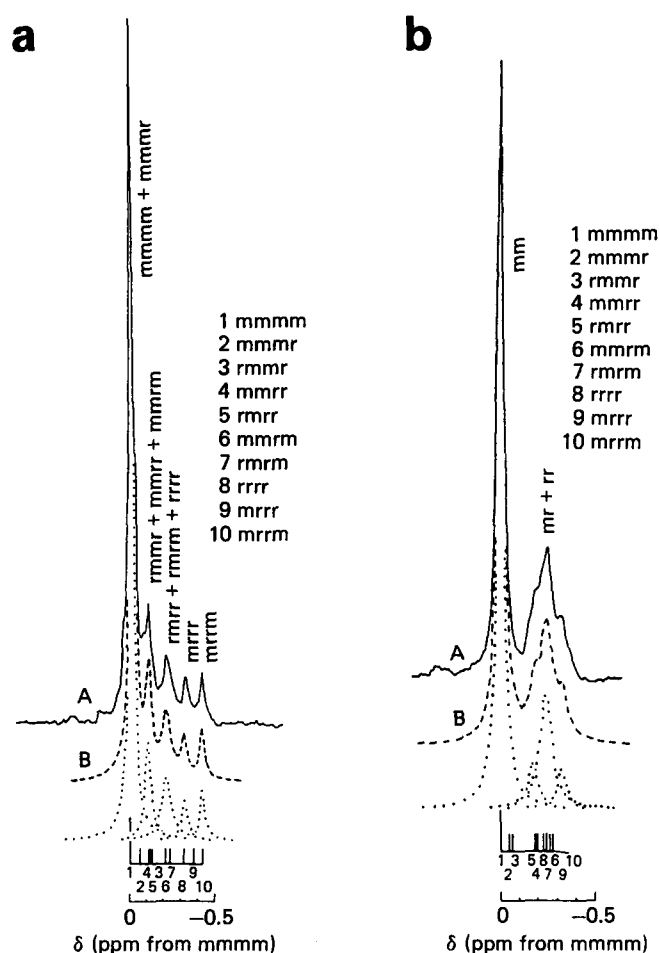


Figure 2 ¹³C n.m.r. spectra of methyl carbon of the side chain (a) and methine carbon of the backbone chain (b) of PB: A, observed spectrum; B, simulated spectra assuming Lorentzian. The stick spectrum calculated theoretically is also included

Table 1 Analysis of ¹³C n.m.r. data of poly(1-butene). Dyad: m 0.753, r 0.247; triad: mm 0.669, mr 0.188, rr 0.143

| Pentad | Observed | Bernoulli trial ^a | Error | First-order Markov ^b | Error | Second-order Markov ^c | Error | Bicatalytic sites model ^d | Error |
|----------------|----------|------------------------------|--------|---------------------------------|--------|----------------------------------|--------|--------------------------------------|--------|
| mmmm | 0.583 | 0.321 | 0.262 | 0.514 | 0.069 | 0.580 | 0.003 | 0.585 | -0.002 |
| mmmr | 0.079 | 0.211 | -0.132 | 0.145 | -0.066 | 0.097 | -0.018 | 0.079 | 0.000 |
| rmmr | 0.007 | 0.035 | -0.028 | 0.007 | 0.000 | 0.004 | -0.003 | 0.019 | -0.012 |
| mmrm | 0.036 | 0.211 | -0.175 | 0.065 | -0.029 | 0.038 | -0.002 | 0.032 | 0.004 |
| mmrr | 0.078 | 0.069 | 0.009 | 0.099 | -0.021 | 0.070 | 0.008 | 0.085 | -0.007 |
| rmmr | 0.032 | 0.069 | -0.037 | 0.009 | 0.023 | 0.027 | 0.005 | 0.038 | -0.006 |
| rmrr | 0.042 | 0.023 | 0.019 | 0.065 | -0.023 | 0.050 | -0.008 | 0.046 | -0.004 |
| mrrm | 0.043 | 0.035 | 0.008 | 0.022 | 0.021 | 0.028 | 0.015 | 0.042 | 0.001 |
| mrrr | 0.045 | 0.023 | 0.022 | 0.068 | -0.023 | 0.069 | -0.024 | 0.046 | -0.001 |
| rrrr | 0.055 | 0.004 | 0.051 | 0.052 | 0.003 | 0.043 | 0.012 | 0.054 | 0.001 |
| s ^e | | | 0.117 | | 0.037 | | 0.013 | | 0.005 |

^a 4mmrr/(mr)² = 10.9, Pm = 0.753

^b P(m/r) = 0.123, P(r/m) = 0.359

^c Pmm/m = 0.931, Pmr/m = 0.362, Prr/m = 0.553, Prr/m = 0.441

^d α = 0.041, σ = 0.453, ω = 0.705

^e Standard deviation

from the four kinds of carbon peaks agree very well with each other, supporting the validity of assignment performed on the basis of the chemical shift calculations⁴.

Using the relative intensities at the pentad level, the polymerization mechanism of PB was examined. Fitting to symmetric Bernoullian, first- and second-order Markovian polymerization models¹¹ was tried. In addition, the bicatalytic sites model of Pino⁸ was examined. In this model, at one site the stereospecific propagation proceeds according to symmetric Bernoullian statistics, and at the other it proceeds under the control of an enantiomorphic model based on the assumed presence of equal numbers of D- and L-preferable catalyst sites, namely, asymmetric Bernoullian. The calculated values are also summarized in Table 1 together with the optimal values of the probability. Among Bernoullian, first- and second-order Markovian models, the last model with a standard deviation of 0.013 is the most appropriate. The bicatalytic sites model with a standard deviation of 0.005 is, however, better than any Markovian model. For the bicatalytic sites model, the

best values of α , σ and ω ¹² were determined as 0.041, 0.453 and 0.705, respectively, where α is the probability to select a D-unit at a D-preferring site in the enantiomorphic site, σ is the probability to select a meso-dyad configuration in the Bernoullian site and ω is the weight fraction of the polymer produced according to the enantiomorphic site model in PB. The polymerization mechanism of this PB can, therefore, be described with the bicatalytic sites model as well as PP⁹.

Finally, the time-averaged random-coil conformation of PB in solution was examined from the bond probabilities used for the chemical shift calculation of each configuration compared with those calculated for PP⁴. The bond probabilities of the 6–11 bonds of 2,4,6,8,10,12,14,16,18-nonamethylnonadecane (a PP model) and those of 2, 4, 6, 8, 10, 12, 14, 16, 18-nonaethylnonadecane (a PB model) are listed for *trans* and *gauche* conformations in Tables 3 and 4, respectively. The fraction of *trans* conformation decreases in the PB model compared with that in the PP model because of a decrease in the values of τ^* , where τ^* takes into account that when both adjacent backbone bonds are *trans* an additional repulsive interaction exists between the ethyl groups of the side chain and backbone. The value of τ^* is equal to unity for PP but 0.6 for PB. In addition, the introduction of racemic units in each configuration of both model compounds leads to increase of the fraction of *trans* conformation and thus decrease of the *gauche* fraction.

REFERENCES

- 1 Ando, I. and Asakura, T. 'Annual Reports on NMR Spectroscopy', (Ed. G. A. Webb), Academic Press, New York, 1980, Vol. 10A, p. 81

Table 2 Relative intensities of the methyl and methylene (side chain) pentads of poly(1-butene)

| | Methyl pentad | Methylene (side-chain) pentad |
|------|---------------|-------------------------------|
| mmmm | 0.661 | 0.662 |
| mmmr | | |
| rmmr | | |
| mmrr | | |
| mmrm | 0.120 | 0.121 |
| rmrr | | |
| rmrm | | |
| rrrr | | |
| mrrr | 0.124 | 0.129 |
| mrrm | | |
| rrrr | 0.047 | 0.045 |
| mrrm | 0.048 | 0.043 |

Table 3 Conformational probabilities of 6–11 bonds of 2,4,6,8,10,12,14,16,18-nonamethylnonadecane

| Pentad | <i>t</i> -6 ^a | <i>g</i> -6 ^b | <i>t</i> -7 | <i>g</i> -7 | <i>t</i> -8 | <i>g</i> -8 | <i>t</i> -9 | <i>g</i> -9 | <i>t</i> -10 | <i>g</i> -10 | <i>t</i> -11 | <i>g</i> -11 |
|--------|--------------------------|--------------------------|-------------|-------------|-------------|-------------|-------------|-------------|--------------|--------------|--------------|--------------|
| mmmm | 0.495 | 0.340 | 0.448 | 0.381 | 0.463 | 0.366 | 0.469 | 0.360 | 0.441 | 0.388 | 0.510 | 0.329 |
| mmmr | 0.550 | 0.033 | 0.444 | 0.394 | 0.466 | 0.372 | 0.514 | 0.330 | 0.395 | 0.449 | 0.660 | 0.214 |
| rmmr | 0.715 | 0.171 | 0.391 | 0.461 | 0.517 | 0.335 | 0.512 | 0.339 | 0.395 | 0.456 | 0.706 | 0.179 |
| mmrm | 0.424 | 0.423 | 0.639 | 0.231 | 0.549 | 0.321 | 0.556 | 0.314 | 0.634 | 0.237 | 0.443 | 0.408 |
| mmrr | 0.502 | 0.348 | 0.560 | 0.295 | 0.464 | 0.391 | 0.613 | 0.259 | 0.633 | 0.240 | 0.587 | 0.283 |
| rmrm | 0.533 | 0.334 | 0.593 | 0.281 | 0.582 | 0.292 | 0.577 | 0.297 | 0.590 | 0.284 | 0.550 | 0.320 |
| rmrr | 0.647 | 0.234 | 0.552 | 0.318 | 0.566 | 0.304 | 0.561 | 0.308 | 0.550 | 0.320 | 0.659 | 0.222 |
| mrrm | 0.440 | 0.414 | 0.665 | 0.213 | 0.651 | 0.229 | 0.654 | 0.226 | 0.669 | 0.210 | 0.431 | 0.422 |
| mrrr | 0.521 | 0.344 | 0.645 | 0.234 | 0.638 | 0.242 | 0.633 | 0.246 | 0.640 | 0.239 | 0.585 | 0.331 |
| rrrr | 0.632 | 0.247 | 0.617 | 0.261 | 0.618 | 0.260 | 0.615 | 0.262 | 0.614 | 0.264 | 0.640 | 0.240 |

^a *t*-6 indicates *trans* conformation of 6 bond

^b *g*-6 indicates *gauche* conformation of 6 bond

Table 4 Conformational probabilities of 6–11 bonds of 2,4,6,8,10,12,14,16,18-nonaethylnonadecane

| Pentad | <i>t</i> -6 ^a | <i>g</i> -6 ^b | <i>t</i> -7 | <i>g</i> -7 | <i>t</i> -8 | <i>g</i> -8 | <i>t</i> -9 | <i>g</i> -9 | <i>t</i> -10 | <i>g</i> -10 | <i>t</i> -11 | <i>g</i> -11 |
|--------|--------------------------|--------------------------|-------------|-------------|-------------|-------------|-------------|-------------|--------------|--------------|--------------|--------------|
| mmmm | 0.479 | 0.352 | 0.444 | 0.383 | 0.454 | 0.373 | 0.465 | 0.364 | 0.433 | 0.394 | 0.497 | 0.337 |
| mmmr | 0.519 | 0.322 | 0.440 | 0.393 | 0.455 | 0.378 | 0.498 | 0.340 | 0.396 | 0.438 | 0.597 | 0.259 |
| rmmr | 0.637 | 0.227 | 0.392 | 0.446 | 0.498 | 0.345 | 0.490 | 0.352 | 0.400 | 0.437 | 0.623 | 0.239 |
| mmrm | 0.406 | 0.428 | 0.593 | 0.261 | 0.506 | 0.345 | 0.518 | 0.334 | 0.586 | 0.269 | 0.429 | 0.299 |
| mmrr | 0.465 | 0.373 | 0.529 | 0.315 | 0.448 | 0.393 | 0.554 | 0.299 | 0.571 | 0.284 | 0.520 | 0.329 |
| rmrm | 0.482 | 0.365 | 0.551 | 0.304 | 0.538 | 0.317 | 0.526 | 0.327 | 0.545 | 0.309 | 0.503 | 0.347 |
| rmrr | 0.560 | 0.297 | 0.510 | 0.340 | 0.527 | 0.327 | 0.513 | 0.336 | 0.505 | 0.345 | 0.518 | 0.280 |
| mrrm | 0.443 | 0.397 | 0.578 | 0.278 | 0.565 | 0.291 | 0.572 | 0.285 | 0.585 | 0.272 | 0.430 | 0.409 |
| mrrr | 0.476 | 0.369 | 0.570 | 0.286 | 0.563 | 0.294 | 0.572 | 0.303 | 0.585 | 0.297 | 0.497 | 0.350 |
| rrrr | 0.550 | 0.305 | 0.545 | 0.310 | 0.546 | 0.309 | 0.540 | 0.314 | 0.538 | 0.316 | 0.563 | 0.293 |

^a *t*-6 indicates *trans* conformation of 6 bond

^b *g*-6 indicates *gauche* conformation of 6 bond

- | | | | |
|---|---|----|--|
| 2 | Schilling, F. C. and Tonelli, A. E. <i>Macromolecules</i> 1980, 13 , 270 | 7 | Asakura, T. and Doi, Y. <i>Macromolecules</i> 1983, 16 , 786 |
| 3 | Zambelli, A., Locatelli, P., Provasoli, A. and Ferro, D. R. <i>Macromolecules</i> 1980, 13 , 267 | 8 | Pino, P. and Mullaup, R. <i>Angew. Chem., Int. Ed. Engl.</i> 1980, 19 , 875 |
| 4 | Asakura, T., Omaki, K., Zhù, S.-N. and Chûjô, R. <i>Polym. J.</i> 1984, 16 , 717 | 9 | Zhù, S.-N., Yang, X.-Z. and Chûjô, R. <i>Polym. J.</i> 1983, 15 , 859 |
| 5 | Zhù, S.-N., Asakura, T. and Chûjô, R. <i>Polym. J.</i> 1984, 16 , 895 | 10 | Nelder, J. A. and Mead, R. <i>Comput. J.</i> 1965, 7 , 308 |
| 6 | Kato, Y., Ando, I. and Nishioka, A. <i>Kobunshi Ronbunshu</i> 1975, 32 , 200 | 11 | Bovey, F. A. 'High Resolution NMR of Macromolecules', Academic Press, New York, 1972 |
| | | 12 | Chûjô, R. <i>Kagaku</i> 1981, 38 , 420 |